ACTA CHEMICA SCANDINAVICA 21 (1967) 1695–1713

Adiabatic Calorimeter for the Investigation of Reactive Substances in the Range from 25 to 775°C. Heat Capacity of α-Aluminum Oxide

FREDRIK GRØNVOLD

Kjemisk Institutt A, Universitetet i Oslo, Blindern, Oslo 3, Norway

An adiabatic calorimeter for measurements of heat capacities, enthalpies of transformation and of fusion for reactive substances in the temperature range 25 to 775°C with an accuracy of about 0.3 % has been constructed. The sample container of vitreous quartz is cylindrical, 3 cm in outside diameter and 12 cm high, with a central well for resistance thermometer and heater. About 50 cm^3 sample material goes into the quartz container which is sealed after filling. It fits into a silver cylinder of 0.5 mm wall thickness with removable bottom. This assembly, with alumina insulated lead wires, is surrounded by three shields of silver (top, side and bottom). The temperature differences between corresponding parts of calorimeter and shields are measured by Pt/90 % Pt 10 % Rh thermopiles, amplified, recorded, and automatically controlled by shield heaters to maintain approximately adiabatic conditions during input and drift periods. The calorimeter and shield systems are surrounded by guard heater bodies of silver and placed in a vertical tube furnace. The temperature of the three guard bodies is controlled to be 0.4°C below the shields and that of the furnace core 10°C lower. The performance of the calorimeter is discussed and heat capacity measurements on α-Al_2O_3 are reported. They show a standard deviation from the mean of 0.15 % and a standard deviation from the NBS data of 0.25 % over the temperature range 27 to 758°C.

Conventional drop calorimetry, in which a heated substance is rapidly transferred to a calorimeter operating around room temperature, is of limited usefulness for studying the energetics of transition and fusion processes in detail. Not only is it difficult to obtain accurate heat capacity data from enthalpy increments over large temperature intervals, but the substance will usually not reach a state of internal equilibrium in the calorimeter. Thus, high temperature phases might be partially retained and crystalline defects frozen in. Under such circumstances adiabatic shield type calorimeters with intermittent heating and temperature equilibration seem unex-

celled for precise work. They have been extensively used in the region below room temperature and have in recent years with the advances in automatic temperature control also become of importance in high temperature calorimetry.[1-5] A survey of the field of high temperature calorimetry has been given recently.[6]

The present calorimeter is the result of experience with several designs over the past seven years. It was intended to be especially useful for the study of transition metal chalcogenides and pnictides, for which vitreous quartz seemed best applicable as sample container. The resulting unfavorably low heat transfer between heating element and substance put strict requirements on adiabatic conditions for obtaining a reasonable accuracy. Experience with the calorimeter indicates that under ordinary conditions accuracies of about 0.3 % are obtained.

The largest part of the uncertainty presumably stems from lack of adiabaticity, but severe problems also arise in measuring temperature differences with the desired accuracy of 1/1000 degree above 600°C. Extensive automation of the temperature controls was necessary to make the operation of the calorimeter a one man job. Special care was taken to provide for easy interchange of samples. The process takes only a few hours and does not require disconnection of any lead wires to calorimeter or shield. Different sources of error have been considered, and the satisfactory operation of the calorimeter tested using a standard sample of α-aluminum oxide.

DESIGN AND OPERATION OF THE CALORIMETER

A. Mechanical construction

Calorimeter proper. The calorimeter proper (*cf.* Fig. 1) is a tube of silver, 30 mm i.d., 128 mm high, 0.5 mm wall thickness, closed at one end and provided with a removable bottom. On its surface are soldered twelve thermocouple pockets for the calorimeter/shield differential thermocouples. Just below the top are located four oval exit tubes at 90° angles, suitable for twin-bore alumina insulators. Four of the eight 0.5 mm diameter Pt wires coming through the insulators are for the resistance thermometer and four for the calorimeter heater. They are led axially down the surface in silver envelopes for about 20 mm and then to the shield system for further temperature equilibration.

The resistance thermometer consists of about 8 m of 0.2 mm diameter platinum wire, helically wound on the surfaces of six alumina tubes, 0.8 mm i.d., 1.2 mm o.d., 100 mm long. These tubes are put into alumina protection tubes, 1.7 mm i.d., 2.7 mm o.d., 100 mm long, which are cemented together around a middle tube of the same diameter. The latter tube is 120 mm long with a 7.5 mm diameter alumina disc at the bottom end and has insulators for fastening the 0.5 mm diameter lead wires at the top.

The calorimeter heater consists of about 0.50 m 0.2 mm diameter Kanthal D wire, threaded through six alumina tubes, 0.8 mm i.d., 1.2 mm o.d., 95 mm long. The alumina tubes are located in the groves between the resistance thermometer protection tubes. To the ends of the wire are welded 0.3 mm

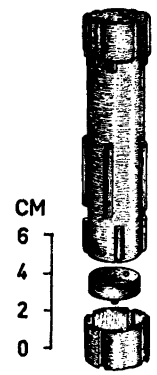

Fig. 1. Calorimeter proper with removable bottom and end covers.

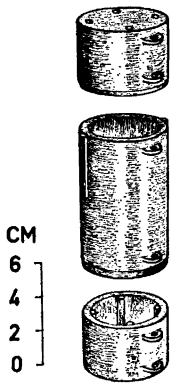

Fig. 2. Top, side, and bottom shield bodies.

diameter Pt wires by means of gold. They are extended by two 0.5 mm diameter wires which are joined again midway between calorimeter and shield.

The substance for which the heat capacity is to be measured is sealed in a clear quartz tube, 29.5 mm outside diameter and 117 mm long. The tube has a central well 9 mm in diameter and 109 mm deep for the heater and temperature sensing elements. This container fits snugly inside the silver calorimeter which can be closed by inserting the loose bottom. The calorimeter is further thermally insulated at both ends by 0.2 mm thick silver covers 34 mm in diameter and 20 mm high with constrictions in order to avoid contact with the thermocouple and lead wire wells on the shields. A 3 mm spacing between calorimeter and top, and bottom covers, respectively, is maintained by crosses made of 90 % Pt 10 % Ir.

Shield system. The calorimeter is surrounded by a shield system made of silver, consisting of a top, side, and bottom part, see Fig. 2. Both the top and the bottom part are closed at the end by 3 mm thick silver plates. For all three shields the heater windings are located axially in a 2.25 mm wide space between two concentric silver tubes of 43.5 and 50 mm internal diameter, respectively, and 1 mm wall thickness. The heater windings of 0.5 mm diameter 90 % Pt 10 % Rh wire go through 46 twin-bore alumina insulators, 23 mm long for the top and bottom shields and 66 mm long for the side shield. On the inside surface of each shield are soldered four pockets for the differential thermocouples. The top shield has in addition four envelopes on its inside and four on the top plate. These envelopes contain alumina tubes for protection of the calorimeter heater and resistance thermometer wires. On the outside of the side shield are two pockets for thermocouples, one Pt/90 % Pt 10 % Rh couple for the absolute temperature, and one reference couple for the guard system. For keeping the shield system in place ears of silver are soldered on the surface of the shields at 180° angle. Two 3 mm diameter stainless steel rods, fastened in the guard top body, go through these ears.

The calorimeter is located in place inside the top and side shields by means of the thermocouple wires which go back and forth between calorimeter and shield. The shield bottom is removable as its thermocouples are fastened to the side shield only and can slide into the proper pockets. Silver wires are soldered on the shield bodies for grounding purposes.

Guard system. Outside the shields is the guard system, see Fig. 3, also consisting of a top, side, and bottom part. The side guard is a cylinder of silver, 62 mm i.d., 90 mm o.d., 140 mm high, in which are drilled six axial holes, three for thermocouples and three for throughgoing stainless steel rods for fastening the top and bottom parts. One of the thermocouple holes goes clear through the side guard body and into the guard bottom in order that the temperature distribution along the guard body might be measured. The cylinder has grooves on its surface for accommodating a heater element which consists of 3.5 m0.5 mm diameter Nichrome wire in twin-bore alumina insulators. The surface of the guard side cylinder is covered by a 0.2 mm thick silver sheet.

The guard top is made from two cylindrical silver plates, 90 mm in diameter, 10 and 7 mm thick, respectively, with a heater element of 1.5 m 0.5 mm diameter 90 % Pt 10 % Rh wire in twin-bore alumina insulators in between. Ten holes are drilled through it for the heater and temperature measuring leads.

The guard bottom is a cylindrical silver plate with a 15 mm high and 14 mm thick wall which, when removed, facilitates the insertion of the calorimetric

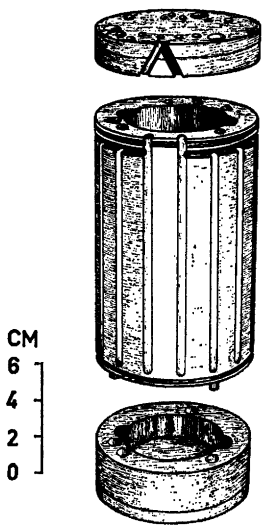

Fig. 3. Top, side, and bottom guard bodies.

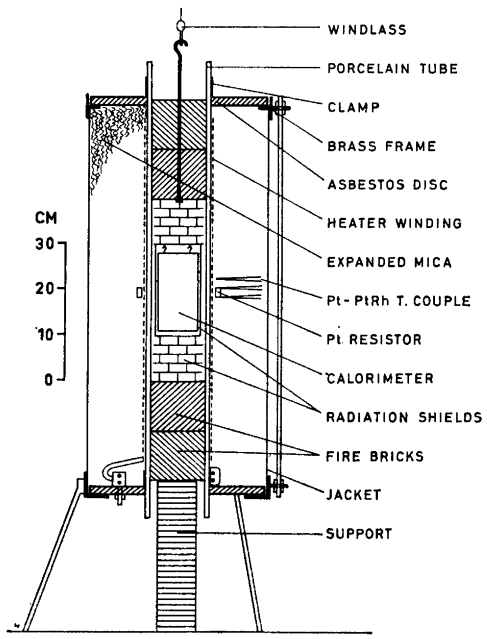

Fig. 4. Calorimeter thermostat.

sample and shield bottom. A heater similar to the guard top one is inserted in the bottom and covered by a 7 mm thick silver plate. Thermocouple wells are drilled to the center both of the bottom and top guard bodies.

Thermostat. The calorimeter system is enclosed in a stainless steel container with radiation shields and light firebrick insulation inside a vertical tube furnace, see Fig. 4. The furnace heater element consists of a 36 m Kanthal A strip, 7 × 0.7 mm², bifilarly wound on a 144 mm diameter porcelain tube (Pythagoras) and connected to the 230 V AC mains through a saturable inductor that can vary the input to the thermostat between 50 and 2500 W. This furnace core is mounted in a casing, 40 cm in diameter, 85 cm long, filled with expanded mica (Vermiculite).

B. Measuring and control circuits

Thermostat. Close to the heater windings of the thermostat is located a Pt/90 % Pt 10 % Rh thermocouple for controlling its temperature by means of a bridge circuit, see Fig. 5. The reference emf can either be that of a thermocouple located in the calorimeter shield or guard body, or a preset emf from a Zener diode potentiometer. The opposing emf's are amplified in a null detector (Leeds & Northrup Model 9834-2) and fed into a current adjusting type controller (Leeds & Northrup Model 10877). The output is amplified and used for governing a 2.5 kW saturable inductor. A small adjustable emf is introduced into the thermocouple circuit to keep the temperature of the thermostat below that of the guard body at all times, usually 10.0 ± 0.5°C. This is easily effected, since the regulating power is about 1000 W °C^{-1}, and the control system does not start to oscillate unless it is adjusted to respond to temperature changes less than 0.05°C.

During the heating-up period the current to the furnace is usually supplied by a Variac for safety reasons and is switched over to the saturable inductor in due time before the experiments are begun, either manually or by a timer. An on-off timer allows the heating to be started at a desired time. To prevent overheating, a thermocouple control circuit is installed, which operates a safety switch when the temperature exceeds a prescribed limit.

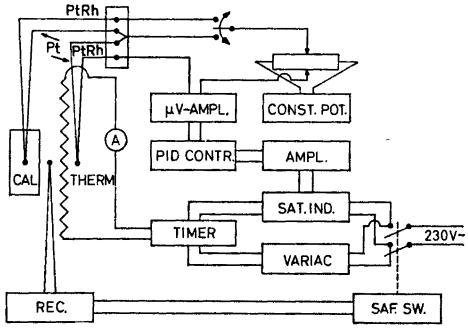

Fig. 5. Thermostat control circuit diagram.

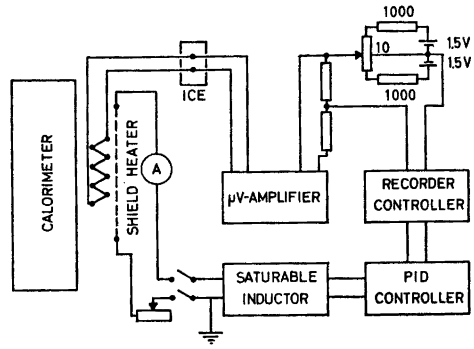

Fig. 6. Shield control circuit diagram.

Guard system. The temperatures of the three guard bodies are kept about 0.4°C below the shield temperature at all times. A temperature gradient of this order is needed for the shield control units to operate satisfactorily. The temperature regulation is accomplished by proportional control systems using as a reference the emf from a thermocouple located in the side shield. The voltage differences are fed into null detectors (Leeds & Northrup Model 9834-1) and the output used for governing saturable inductors. The maximum rectified currents in the top and bottom guard heaters are 2 A, and in the side heater 4 A.

Shield system. The calorimeter/shield difference thermopiles consist of eight junctions of Pt/90 % Pt 10 % Rh wire, of which the alloy wires are used as lead wires because of their greater mechanical strength. The measuring and control circuits, see Fig. 6, are made up of commercially available components. The thermocouple leads go into an ice-bath, and the outgoing copper leads are connected to microvolt amplifiers (Liston-Becker Model 8A for the side shield and Leeds & Northrup Model 9835-B for the top and bottom shields). The output is adjusted to Speedomax G and Speedomax H recorder-controllers, respectively, having externally variable control point changers. The amplification is adjusted so that the full recorder scale corresponds to 50 μV. Control action is effected by current adjusting type instruments (Leeds & Northrup Model 10877) with output matched to a saturable inductor giving a maximum current of 2 A through the 17 ohm shield side heater element. For top and bottom shields the maximum currents are 1 A and the heater resistances about 6 ohm. The operation of the controllers is based upon three different modes of action, (1) the proportional action, which changes the power supplied to the shield by an amount proportional to its temperature difference from the calorimeter, (2) the reset or integral action, which gradually reduces the average of this temperature difference to zero, and (3) the rate or derivative action, which keeps the time response of the controller as short as possible without causing sustained temperature oscillations (hunting).

Grounding of one side of the shield heater windings and application of rather low voltages were essential for successful high temperature operation of the shield control circuits. The control system is capable of holding the emf of the thermopiles within 0.3 μV at temperatures up to about 750°C. This corresponds to between 0.008 and 0.013°C depending upon the temperature, except at the beginning and end of the energy input period where the maximum deviations are about ten and five times as large, respectively.

Energy input. The energy inputs are determined by measuring the current through the heater, the potential drop across it and the input time. A schematic wiring diagram is shown in Fig. 7.

The electrical energy comes from four 6 V heavy-duty lead, storage batteries connected in series. The current goes through a resistor, adjustable in seven steps (0, 12.5, 25, 50, 75, 100, and 150 ohms), a standard resistor of 0.010000_0 abs. ohms, an ammeter (0—1 A) for indication purposes, and either through the calorimeter heater (CAL) or the dummy heater (DUM) of approximately equal resistance, depending upon the position of a relay. In this way very stable discharge conditions prevailed, the main disturbance coming

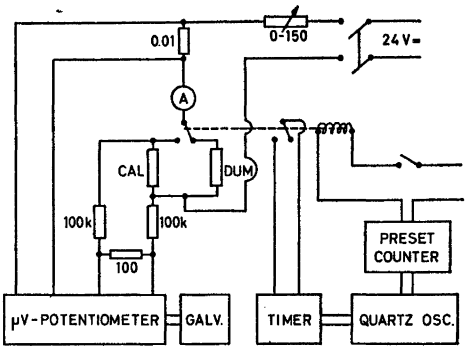

Fig. 7. Energy input circuit diagram.

from the increase in resistance of the calorimeter heater in the beginning of the input period before approximately steady state heat transfer conditions are created. By making the heater resistance about 50 % of the total resistance in the circuit, the power will not vary appreciably even though the calorimeter heater resistance changes. Experiments indicate that for a heating current of 0.4 A the average increase in resistance during a 10°C input is about 0.1 % and the corresponding change in power less than 0.05 % for a well charged battery.

In shunt with the calorimeter heater are two 100 000 ohm resistors and a 99.998 abs. ohm standard resistor, the total resistance being 200 123 abs. ohm at 25°C and increasing to 200 124 abs. ohm at 750°C. The potential drops across the 99.998 ohm shunt resistor and the previously mentioned 0.01 ohm series resistor are measured with a double six dial microvolt potentiometer (Rubicon Model 2773) and a calibrated standard cell. The potentiometer dial readings are recorded by means of a printer (Beckman Model 1453).

The calorimeter heater is operated by a counter controller (Beckman Model 7416) with a double pole double throw mercury relay, which also operates the clutch of an electric timer (Jaquet 0.01 sec/division). The controller and timer are both run by a quartz crystal oscillator (Rohde und Schwarz Type XSC). The accuracy of the time indication has been tested with a frequency timer (Beckman Model 5571) connected to the calorimeter heater, and found to be within 0.01 sec for times up to 100 sec and within 0.01 % for longer times.

Calorimeter temperature. In the earlier versions of the calorimeter, temperatures were measured by means of a 90 % Pt 10 % Rh resistance thermometer, but after considerable experimentation a platinum resistance thermometer was developed, which showed the necessary stability under continued use up to 800°C.

The resistance of the platinum thermometer is related to the International Practical Temperature Scale [7] by the equation

$$T = \frac{R_T - R_0}{\alpha R_0} + \delta \left(\frac{T}{100} - 1 \right) \frac{T}{100}$$

devised by Callendar, in which T is the temperature, R_0 and R_T the resistance at zero and T°C, respectively, α and δ constants for the particular thermometer.

The constant α is determined from calibrations at the ice and steam defining fixed points, and must be greater than 0.003920 in order to satisfy one of the requirements for a standard resistance thermometer. The constant δ is determined from a calibration of the thermometer at the melting point of zinc, 419.505°C, which is a recommended fixed point on the International Practical Temperature Scale.

While the values of R_0 and α were determined for the thermometer before installation in the calorimeter, the value of δ was determined by introducing a small, sealed sample of pure zinc into the calorimeter and observing its melting point. Further experiments using also tin, lead, and antimony were performed to check the constancy of the thermometer. In addition, a removable, calibrated Pt/90 % Pt 10 % Rh thermocouple in the side guard body allows checking of the calorimeter temperature.

Temperatures calculated from the resistance values by means of the above equation and its constants have only been subject to small corrections for deviations from the International Practical Temperature Scale as represented by the melting point standards. The corrections have not amounted to more than 0.1°C at any temperature during the years of operation. For most of the data reported the resistance measurements were made on a Mueller bridge (Leeds & Northrup Model 8072) with digital read-out.

C. Experimental procedure

By means of a suitable current through the heater windings of the calorimeter thermostat the temperature is maintained about 10°C below the desired beginning temperature of the experiments. Crushed ice is supplied to the cold junctions of the thermocouples, and the electrical instruments put into operating condition. The calorimeter is then heated about 10°C over a 6—16 min interval and the shield and guard temperature regulators switched over to automatic control. After some time the control zero on all three shield units is shifted in order to minimize the drift rate of the calorimeter, as observed from readings on the Mueller bridge every minute. When the drift rate is steady and less than 0.0005 ohm, or 0.005°C, over a 5 min interval a reversed reading on the Mueller bridge is taken and the first ordinary input is begun one minute later.

The operator takes readings of the heater potential and current about every minute. Usually after 6—16 min the calorimeter current is switched back to the dummy heater, and when the calorimeter temperature approaches its new equilibrium value the operator starts taking readings on the Mueller bridge again. Under ordinary conditions, *i.e.* when no transitions take place in the sample, the calorimeter reaches equilibrium after about 30 min in the room temperature range, after about 20 min at 300°C and within 10 min at 750°C. The drift rate is observed over a 5 min interval, a reversed reading taken on the Mueller bridge, and a new input started. Results of a typical heat-capacity run are shown in Table 1.

Table 1. Recording of a heat-capacity run. (α-Al_2O_3, Series VII input 12).

Time, min	Resistance, ohm	Time, min	Potential, current
45.0	94.7005 N	63.0	0.31717 A
46.0	94.7002 N	64.0	3.7963 V/2
47.0	94.7000 N	65.0	0.31715 A
48.0	94.6993 N	66.0	3.7963 V/2
49.0	94.6992 N	67.0	0.31712 A
50.0	94.6993 N	68.0	3.7964 V/2
51.0	94.6992 N	69.0	0.31708 A
52.0	94.6991 N	70.0	3.7964 V/2
53.0	94.6991 N	71.0	0.31706 A
54.0	94.6992 N	71.9	3.7964 V/2
55.0	94.6776 R	72.0	Input 12 stop, input time:
56.0	Input 12 start		960.085 sec
	Potential, current		Resistance, ohm
56.5	3.7956 V/2	80.0	95.6496 N
57.0	0.31728 A	81.0	95.6491 N
58.0	3.7959 V/2	82.0	95.6487 N
59.0	0.31722 A	83.0	95.6487 N
60.0	3.7961 V/2	84.0	95.6487 N
61.0	0.31719 A	85.0	95.6486 N
62.0	3.7962 V/2	86.0	95.6484 N
		87.0	95.6485 N
		88.0	95.6256 R
		89.0	Input 13 start

D. Derivation and accuracy of data

The heat capacity, C, of a system at any temperature, T, can be defined as

$$C(T) = \lim(\Delta Q/\Delta T), \text{ when } \Delta T \rightarrow 0$$

where ΔT is the temperature change associated with introduction (or removal) of a quantity of heat ΔQ. The accuracy to which a heat capacity can be determined is thus limited by experimental difficulties in temperature measurements and by the inherent difficulties in making the heat flow conditions amenable to calculation. Above 500°C an accuracy of 1 % must be considered as rather good, and one of 0.1 % has apparently not yet been achieved. Thus, while the detection of temperature increments of 0.001°C at 500°C offers no unsurmountable difficulties, uncertainties about the heat flow conditions severely limit the accuracy of the results.

A precise determination of the quotient $\Delta Q/\Delta T$ can be obtained by applying heat leak corrections to the measured energy input to give ΔQ_{corr} corresponding to ΔT_{obs}. Alternatively, it might be obtained by correcting the temperature increase instead of the energy input. If the former approach is adopted, and the temperature gradient between the calorimeter and its surrounding shields is small enough for Newton's law of heat transfer to be applicable, one has:

$$\frac{\Delta Q}{\Delta T} = \frac{\Delta Q_{obs} + a\,C\int_{t_i}^{t_f} dt + k\int_{t_i}^{t_f} \theta\, dt}{T_f - T_i}$$

Here ΔQ_{obs} is the electrical energy dissipated, $a = dT/dt$ is the intrinsic temperature drift of the calorimeter under "equilibrium" conditions, k is the heat conductance between calorimeter and shield, θ the temperature excursions of the shield from the control zero, C is the heat capacity of the calorimeter and its contents, t_i and t_f the times at which steady state temperatures T_i and T_f are observed before and after an energy input. Obviously, a, k, and C are temperature-dependent, and θ time-dependent. The determination of the different terms in the above equation with comparable accuracy will now be considered in more detail.

The energy input, ΔQ_{obs}, can be evaluated in terms of the equation

$$\Delta Q_{obs} = \int V\, i\, dt \quad \text{joule}$$

where V is the potential drop across the calorimeter heater in volt, i the current through the heater in ampere, and t the time, measured in seconds. For ordinary heat-capacity runs of 6—16 min duration the potential and current measurements are taken as the average of readings on the microvolt potentiometer, multiplied by the proper conversion factors. This averaging procedure might be compared with a strict integration procedure of the instantaneous power product obtained from many closely spaced voltage and current measurements, and the method of Gibson and Giauque [8] of measuring the current at 21 and 79 % of the elapsed input time and the potential at half-time. In typical experiments the three methods were found to give the same result within 0.01 %, and the averaging method is thus satisfactory. The Rubicon microvolt potentiometer was not found to have errors in excess of 0.01 % and the accuracy of readings to this precision is therefore only dependent upon knowledge of the emf of the standard cell, and especially its variation with time. For the working standard cell (Weston No. 14473) several calibrations over the years 1955—1963 have shown a total decrease of only 0.022 % in its emf.

A very small additional amount of heat is introduced by the measuring current of 2 mA in the resistance thermometer. Over a 10 min period it amounts to about 0.07 joule at room temperature and increases to 0.25 joule at 800°C. For ordinary energy inputs of about 1500 joules the correction is therefore negligible, but not for small energy inputs. The importance of this additional energy of the temperature drift of the calorimeter will be considered below. No correction for the heat generated in the heater leads is applicable, since the potential leads branch off from the current leads in the middle between calorimeter and shield and the heat transfer coefficient between the wires and calorimeter is practically equal to that between the wires and shield.

The drift correction, $\int a\,C\,dt$, contains a factor $a = dT/dt$, the temperature drift of the calorimeter under "equilibrium" conditions, *i.e.*, when minimum heat exchange with the surroundings takes place. This drift rate can, of course, only be measured before and after each experiment and is noted from measurements of the thermometer resistance on the Mueller bridge to

the nearest 0.0001 ohm every minute until a steady state condition prevails over a 5 min interval. No reversed reading on the Mueller bridge is taken in this period, since that was found to make the drift rate observations more uncertain, presumably because of slight build-up of charges on the materials supporting the platinum resistor. The error introduced from changes in the inequality of the lead resistances, and thus in the normal and reversed readings on the Mueller bridge over a 5 min time interval for a temperature change of the order of 0.005°C was found negligible in this connection. The precision of the G-4 Mueller bridge is sufficient for avoiding any errors in the resistance measurements in excess of 0.0001 ohm.

Fluctuations in the control zero of the shield control units are a limiting factor in the determination of the drift rate. At room temperature the sensitivity of the calorimeter/shield thermopiles is 25 $\mu V°C^{-1}$, increasing to about 40 $\mu V°C^{-1}$ at 400°C and above. The zero-point stability of the microvolt amplifiers is of the order $\pm$ 0.1 $\mu V\ h^{-1}$, which implies that the temperatures of the shields can only be controlled to about $\pm$ 0.003°C over a period comparable to that of two successive drift periods. To estimate the error from this source let it be assumed that all three shields are controlled 0.003°C too hot. At 1000°K the heat transfer between calorimeter and shields, see below, is 0.43 $W\ °C^{-1}$. The transferred energy is thus 0.08 joule min^{-1}, which for the loaded calorimeter corresponds to a temperature drift of 0.0005°C min^{-1}. The average drift rate from this uncontrollable source is estimated to be half of the above value and the transferred energy is 0.04 joule min^{-1}.

A small additional uncertainty in the drift rate determination stems from the heat generated in the resistance thermometer. It varies, as already mentioned, between 0.07 and 0.25 joule over a 10 min period and results in a temperature increase of about 0.0001°C min^{-1} for the empty calorimeter.

In the earlier version of the calorimeter, systematically changing values for the drift rate before and after an energy input of the order + 0.0002°C min^{-1} were usually observed, unless the control point zero of the calorimeter/shield thermopiles were shifted. Apparently, the absolute temperature of the calorimeter was of importance for this drift, probably because of some small openings in the shield system for the supporting quartz rods, which allowed a slight heat transfer between calorimeter and more distant surroundings to take place.

Under such conditions the drift correction was calculated according to the formula

$$(C/5)(T_i - T_{i-5})(2 + t/2) + (C/5)(T_f - T_{f+5})(t_f - t_i - 2 - t/2) \text{ joule}$$

where C is the heat capacity of the calorimetric system, T_i the temperature of the calorimeter at time t_i, *i.e.* 2 min before input start, T_{i-5} its temperature 5 min earlier, t the input time in minutes, T_f the temperature of the calorimeter after equilibration at time t_f, and T_{f+5} the temperature of the calorimeter 5 min later.

The applied corrections have not exceeded 0.2 % for the measurements reported here. For the new calorimeter, only random fluctuations in the calorimeter temperature seem to occur under ordinary conditions, and drift corrections have therefore in general not been applied.

In addition to the heat transfer observable as calorimeter drift, further heat transfer is possible in the input period and the first part of the equilibration period. It can only be taken into account by observing the apparent temperature difference between calorimeter and shields as a function of time. This temperature difference, θ, and its time integral are observable on the recorder charts of the three shield control units. Thus, by separate determinations of the heat transfer between calorimeter and shields as a function of temperature it is possible to evaluate that part of the heat transfer between calorimeter and shields which takes place during the temperature rise of the calorimeter.

To obtain the small corrections for the observed deviations of the shield temperatures from the calorimeter temperature, heat transfer calculations and measurements have been carried out. In the calculations the heat transfer by convection was neglected due to its relatively smaller importance than heat transfer by conduction and radiation.

Between the calorimeter and side shield the conduction is by air and by the differential thermocouples. The solid conduction is mainly caused by the eight thermocouple wires that connect calorimeter and side shield. The heat flow rate is obtainable directly from the basic equation

$$\frac{dQ}{dt} = -k A \frac{d\theta}{dx}$$

where k is the thermal conductivity of the solid substance, A its area perpendicular to the heat flow, and $d\theta/dx$ the temperature gradient. For platinum $k = 0.4$ W cm^{-1} °C^{-1} at room temperature, the diameter of the wires is 0.5 mm and the length over which the heat is conducted amounts to 11 mm. An additional heat flow of about 0.03 W °C^{-1} goes through the alumina insulators surrounding the wires.

The heat flow rate by radial air conduction through a cylinder of finite length and perfectly insulating ends can be expressed as (see for example Jacob [9])

$$\frac{dQ}{dt} = k L 2 \pi \frac{\theta}{\ln(r_1/r_2)}$$

where k is the thermal conductivity of air, varying from 0.00024 W cm^{-1} °C^{-1} at 300°K to 0.0006 W cm^{-1} °C^{-1} at 1100°K, L is the length of the cylinders of radii r_1 and r_2, and θ the temperature difference between these two cylinder surfaces.

The rate of heat transfer by radiation was calculated from the equation

$$\frac{dQ}{dt} = \frac{\sigma e_1 A_1 (T_1^4 - T_2^4)}{1 + e_1[(1/e_2) - 1](A_1/A_2)}$$

where $e_1 = e_2$ is the emissivity of silver, taken to be 0.07, A_1 and A_2 the areas of the internal and external cylinder, respectively, $\sigma = 5.67 \times 10^{-12}$ W cm^{-2} °K^{-4}, T_1 and T_2 the absolute temperatures of calorimeter and shield surface, respectively. With these constants and for small temperature differences $\theta = T_1 - T_2$ compared to the absolute temperature

$$\frac{dQ}{dt} = 0.87 \times 10^{-10} T^3 \theta \text{ watt}$$

The different contributions to the heat flow rate coefficient between calorimeter and side shield are shown as function of temperature in Fig. 8a. Similar calculations have been carried out for the heat flow rate between calorimeter and top and bottom shield. Those for the bottom shield are shown in Fig. 8 b. The heat flow rate for the top shield is slightly higher since the

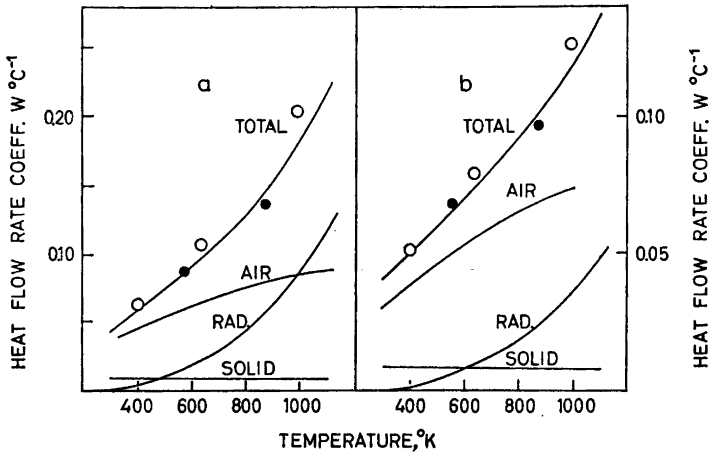

Fig. 8. Heat flow rate coefficients as function of temperature for side shield (a), and bottom shield (b). Solid lines refer to calculations, ● observations for empty calorimeter and O to observations for calorimeter plus sample (α-Al_2O_3).

thermometer and heater leads provide a solid conduction about twice that between calorimeter and bottom shield.

Experimental data on the heat exchange between calorimeter and shield are also included in Fig. 8. They were obtained by shifting the control zero on one shield control unit at a time. Results both with and without sample in the calorimeter are seen to be in good accord with those calculated.

The temperature excursions of the adiabatic shields, as they appear on the recorders, are such that the positive deviation of the calorimeter relative to the shields in the beginning of the heat input period is almost exactly compensated by the negative deviation after the input is over. These unwanted excursions are due to limitations in the action of the shield control units and the relatively long response time of the thermocouples, which is of the order 0.2 min. The composite parts of the excursions usually amount to an energy transfer of about 0.7 joules at room temperature and about 1.5 joules at 775°C.

Additional heat exchange due to gradients set up during the heating period might constitute a source of systematic error in the derived data. Its magnitude is difficult to estimate, and as shown by West,[10,11] it cannot be accounted for by varying the heating rate. In a suitably constructed apparatus the temperature distribution over the calorimeter surface should be the same whether or not the calorimeter is filled with sample. This condition seems reasonably well fulfilled for the present calorimeter, and possible systematic errors should therefore be largely eliminated by subtracting the experimentally obtained data for the empty calorimeter from those of the full.

The temperature differential between shield and guard bodies was found to be non-critical. Even by increasing it to ten times its normal value of 0.4°C the "zero" heat leak of the calorimeter remained practically unchanged. Changing of the temperature differential between thermostat and calorimeter

was more readily noticable, and lowering of the thermostat temperature resulted in a more positive "zero" heat leak of the calorimeter, as long as the guard heaters were able to supply enough heat.

Because of the finite temperature ranges involved, corrections to the values of $\Delta Q/\Delta T$ are required in order to arrive at true heat capacity values. It has been shown by Osborne *et al.*[12] that if the heat capacity can be expressed as a function of temperature, the heat capacity at $T = (T_1 + T_2)/2$ can be approximated as

$$C_T^* = \frac{\Delta Q}{\Delta T} - \frac{(\Delta T)^2}{24} \frac{d^2(\Delta Q/\Delta T)}{dT^2}$$

In the present case the curvature corrections to the heat capacities both for empty and full calorimeters are less than 0.05 %. The pressure dependence of the heat capacity of aluminum oxide at the temperatures in question is negligible, such that C_p^* is equal to C_p°, or C_p.

RESULTS

In order to test the performance of the calorimeter heat capacity measurements were made on a portion of a special sample of aluminum oxide prepared by the U.S. National Bureau of Standards at the request of the IV. Calorimetry Conference in 1948 to serve as a heat capacity standard. Results of high accuracy have been reported by members of the Bureau of Standards [13,14] and other research groups. Most of the data in the high temperature range have been obtained by drop calorimetry. The experimental sample was kindly made available to the author by Drs. Ginnings and Prosen for checking and intercomparison purposes.

First the heat capacity of the calorimeter with enclosed vitreous quartz container was determined as a function of temperature. Hydrogen gas at 10 cm Hg pressure was introduced before sealing the container to insure faster temperature equilibration. Results obtained both for the old calorimeter (Mark II) and the new one (Mark III) are shown in Fig. 9. Estimates (s′) of the standard deviations of the values (x_i) from the smooth data (x_s) over the temperature range 37 to 782°C give $s' = \sqrt{\sum(x_i - x_s)^2/n(n-1)} = 0.33$ % and 0.20 %, respectively.

No variations in specific heat of containers made from different quartz tubes were noted, but heating above 700°C gradually resulted in devitrification of the glass. X-Ray powder photographs taken confirm that the crystalline phase formed is quartz. The heat of crystallization of the glass might not be detected in the experiments, since it leads only to a slight negative drift in the calorimeter temperature, which is not easy to separate from other causes. At 750°C a crystallization rate of the order 0.05 g h^{-1} has been observed, which should result in a temperature drift of the empty calorimeter of −0.002°C min^{-1}, taking the enthalpy of crystallization [15,16] to be −10 kJ $mole^{-1}$ at 750°C. While this effect is compensated for by adjusting the drift to zero, the transition of α-quartz to β-quartz with an enthalpy change [16] of 20 J g^{-1} clearly shows up in the heat capacity curve around 575°C when the container has

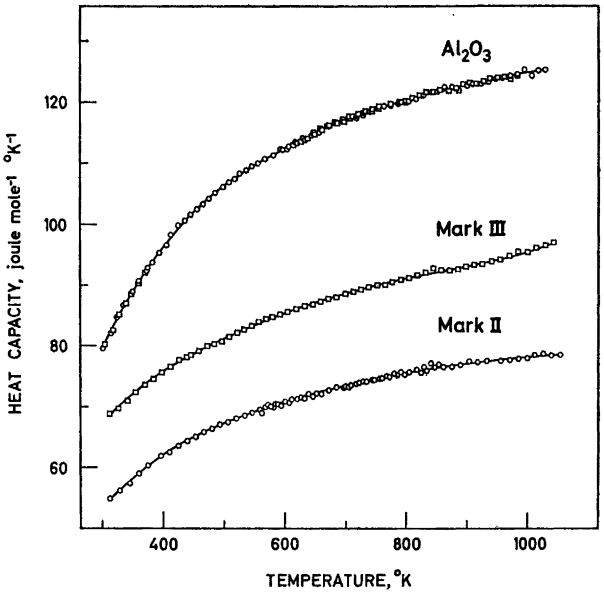

Fig. 9. Heat capacities of aluminum oxide and of empty calorimeters Mark II and Mark III as function of temperature.

been at 750°C for some time. The lower heat capacity of crystalline quartz compared to glass above room temperature is negligible in this connection.

The aluminum oxide sample, weighing 84.756 g *in vacuo*, was sealed into a clear quartz container of about the same weight as the empty one, and with hydrogen gas of 10 cm Hg pressure to improve conduction. The resulting heat capacities are presented in Fig. 9 and Table 2 after subtraction of the values for the empty calorimeter and taking the different amounts of quartz glass in the two sets of experiments into account. The empty calorimeter represented 49.5 % of the total heat capacity at 300°K, decreasing to 48.0 % at 1050°K in case of the Mark III calorimeter, and 53.5 % and 51.3 %, respectively, for Mark III. The estimated standard deviation (s′) of the values from the smooth data is 0.15 % over the temperature range 301 to 1031°K. A similar comparison with the data by Furukawa *et al.*[14] gives s′ = 0.25 %. In the range 300 to 400°K the present data scatter around the curve given by Furukawa *et al.* and agree with the results by West and Ginnings [2] and Trowbridge and Westrum.[5] The definite positive trend found in recent years around room temperature by Romanovskii and Tarasov,[17] Martin,[18] and Edwards and Kington [19] has not been substantiated.

In agreement with the heat capacity data by West and Ginnings,[2] Trowbridge and Westrum,[5] and Martin and Snowdon,[20] the tentative NBS standard values appear to be about 0.2 % low around 500°K (*cf.* Fig. 10). The data obtained by Shmidt and Sokolov [3] do not seem sufficiently accurate to allow

Table 2. Heat capacity data of α-Al_2O_3, joule mole^{-1} °K^{-1}.

T, °K	C_p	ΔC_p [a]	T, °K	C_p	ΔC_p [a]
	Series I		776.72	119.59	−0.05
300.94	79.45	−0.16	788.42	119.97	−0.02
313.56	82.05	−0.17	800.10	120.21	−0.11
325.85	84.84	+0.23			
337.80	86.82	+0.04		Series VI	
349.45	88.89	+0.09	793.24	120.13	0.00
360.91	90.64	−0.01	804.88	120.23	−0.23
372.16	92.30	−0.06	816.48	120.69	−0.09
			828.03	121.23	+0.14
	Series II		839.53	121.33	−0.06
374.36	92.48	−0.20	850.97	121.70	+0.03
382.68	93.78	−0.12	862.37	121.95	0.00
393.57	95.32	−0.05	873.77	122.51	+0.29
404.26	96.67	−0.03	885.16	122.63	+0.15
414.81	98.13	+0.18			
425.21	99.85	+0.73		Series VII	
435.49	100.52	+0.31	888.82	122.13	−0.44
445.67	101.48	+0.23	900.96	122.68	−0.16
455.75	102.43	+0.20	912.99	123.02	−0.07
465.73	103.29	+0.13	924.96	123.39	+0.05
475.62	104.14	+0.11	936.89	123.45	−0.13
485.42	105.21	+0.35	948.77	124.04	+0.23
			960.61	124.12	+0.09
	Series III		972.41	124.45	+0.20
498.21	106.13	+0.23	984.18	124.67	+0.20
507.81	106.99	+0.35	995.93	125.47	+0.80
517.31	107.59	+0.24	1007.67	124.55	−0.37
526.76	108.24	+0.22	1019.39	125.44	+0.38
536.14	108.75	+0.08	1031.06	125.60	+0.35
545.46	109.53	+0.25			
556.28	109.91	−0.07		New calorimeter Series VIII	
568.56	110.72	0.00	303.98	80.39	+0.15
580.76	111.32	−0.14	315.59	82.53	−0.09
592.88	112.35	+0.23	327.15	85.10	+0.27
604.92	112.51	−0.25	338.19	86.91	+0.05
616.88	113.49	+0.12	349.03	88.65	−0.08
628.78	114.17	+0.21	359.69	90.55	+0.08
			370.16	92.09	+0.02
	Series IV				
595.43	112.14	−0.11		Series IX	
606.45	112.64	−0.21	616.05	113.04	−0.29
619.00	113.17	−0.31	626.09	113.67	−0.16
631.47	113.93	−0.16	637.49	114.08	−0.29
643.86	114.60	−0.07	649.94	114.79	−0.16
656.17	115.07	−0.16	662.33	115.52	+0.03
			674.25	116.23	+0.24
	Series V		686.11	116.65	+0.17
710.19	117.49	+0.09	697.91	117.00	+0.06
719.12	117.48	−0.25	709.66	117.55	+0.17
729.54	117.95	−0.15	721.35	117.91	+0.10
741.40	118.52	+0.01	733.00	118.46	+0.24
753.20	119.12	+0.22	744.65	118.86	+0.18
764.97	119.33	+0.06	755.96	119.29	+0.30

Table 2. Continued.

T, °K	C_p	ΔC_p [a]	T, °K	C_p	ΔC_p [a]
	Series X		822.40	121.09	+0.15
648.17	115.18	+0.31	833.82	121.73	+0.51
659.61	115.66	+0.29	845.18	121.74	+0.23
671.76	116.14	+0.25	856.49	122.01	+0.20
683.85	116.76	+0.37			
695.88	117.12	+0.26		Series XII	
707.85	117.62	+0.30	871.73	121.87	−0.31
719.77	117.71	−0.04	883.17	122.37	−0.07
731.65	118.18	+0.01	894.56	123.03	+0.33
743.49	118.58	0.00	905.91	123.11	+0.17
755.28	119.06	+0.10	917.23	123.00	−0.18
			928.51	123.48	+0.07
	Series XI		939.73	123.87	+0.23
776.25	119.56	−0.06	950.90	124.13	+0.28
787.85	120.27	+0.30	962.04	124.13	+0.07
799.41	120.22	−0.08	973.13	124.00	−0.27
811.93	120.77	+0.11	984.18	124.62	+0.15

[a] ΔC_p represents the difference between the observed value and that calculated from the data by Furukawa *et al.*[14]

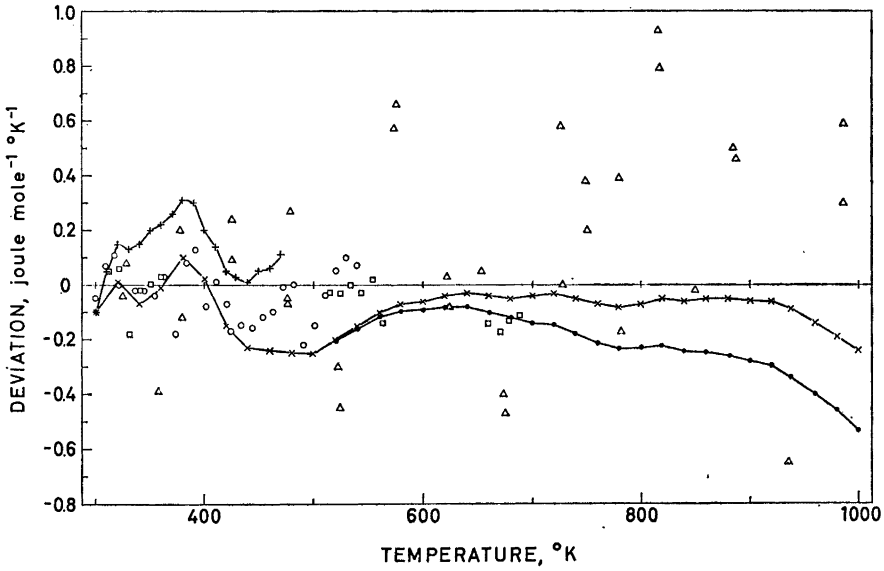

Fig. 10. Deviations in heat capacity from the present smooth curve for aluminum oxide for: □ data by West and Ginnings,[2] ○ data by Trowbridge and Westrum,[5] + — + smooth data by Martin and Snowdon,[20] △ data by Shmidt and Sokolov,[3] × — × smooth data by Furukawa *et al.*,[14] ●——● and as corrected by Ginnings.[21]

any definite conclusions about the deviations in this temperature range, but they show a definite positive trend with increasing temperature. The rather sudden change in sign of the deviations for the present data around 660°K may be fortuitous, but the trend is unmistakably positive in the range 700 to 1050°K and about 0.1 % higher than the NBS data in this range.

The accuracy of the work by Furukawa *et al.*[14] has been questioned by one of the coworkers, Ginnings,[21] on the grounds that the Nichrome V sample container used shows a transition in the range 600 to 700°C. A corrected enthalpy equation is presented which results in a 0.08 % lower enthalpy increment for the region 298 to 1000°K, and a 0.3 % lower heat capacity value at 1000°K. This further deviation of the NBS data from the results obtained here justifies a more thorough study of the high temperature heat capacity of the α-Al_2O_3 standard material. It might be mentioned in this connection that the measurements reported here should not be taken to represent the limiting precision and accuracy obtainable with the instrument, but rather to explore what could be expected with regard to accuracy in the heat capacity measurements on the reactive iron and nickel selenides under study here.

Acknowledgements. The author expresses his appreciation to Professor Haakon Haraldsen for his interest in this study and for making laboratory facilities available, to Professor Edgar F. Westrum, Jr. for the benefit of his experience in calorimetry, to Drs. Defoe C. Ginnings and Ed Prosen for a standard sample of aluminum oxide, and to *Norges Almenvitenskapelige Forskningsråd* for continued support.

The cooperation of Mr. Sverre Nordvik and the firm K. A. Rasmussen in making the silver parts of the calorimeter, and Mr. Olav Norderhaug and N. A. Gasaccumulator in constructing power amplifiers is thankfully acknowledged.

The author would in addition like to thank a number of persons associated with the Department for assistance with constructing and developing the apparatus to its present stage of performance, especially Magne Lein, Amund Helgesen, Tore Eriksen, Torgeir Fløtten, Olav Gjessing, Håkon Mohn and Bjørn Lyng Nielsen. In the time-consuming calibrations, measurements, and reduction of data, both for the present calorimeter and the three earlier versions, a number of persons have taken part. Among these, Nils Erik Askheim, Grete Bendtsen, Karin Bjåmer, Andreas Bugge, Anders Langen, Bjørn Lyng Nielsen, Jan Thorstensen, Torkild Thurmann-Moe, and Tor Tufte were associated with the project for considerable periods of time and their valuable assistance is recognized.

REFERENCES

1. Wallace, W. E., Craig, R. S. and Johnston, W. V. *U. S. At. Energy Comm.* Unclassified Document NYO-6328 (1955).
2. West, E. D. and Ginnings, D. C. *J. Res. Natl. Bur. Std.* **60** (1958) 309.
3. Shmidt, N. E. and Sokolov, V. A. *Russ. J. Inorg. Chem.* **5** (1960) 797.
4. Grønvold, F. Paper presented at the International Calorimetry Conference, Ottawa Aug. 14.—18., 1961.
5. Trowbridge, J. and Westrum, E. F., Jr. *J. Phys. Chem.* **67** (1963) 2381, and personal communication.
6. Grønvold, F. Calorimetry at high temperatures, IAEA Symposium on Thermodynamics, Vienna July 22.—27., 1965.
7. *Comptes rendus, Onzième Conf. Gén. des Poids et Mésures*, Paris 1960; see also *J. Res. Natl. Bur. Std.* **A 65** (1961) 139.
8. Gibson, G. E. and Giauque, W. F. *J. Am. Chem. Soc.* **45** (1923) 93.
9. Jacob, M. *Heat Transfer*, Vol. I and II. Wiley, New York 1949 and 1957.
10. West, E. D. *J. Res. Natl. Bur. Std.* **A 67** (1963) 331.

11. West, E. D. *Trans. Faraday Soc.* **59** (1963) 2200.
12. Osborne, N. S., Stimson, H. F., Sligh, T. S., Jr. and Cragoe, C. S. *U.S. Natl. Bur. Std. Sci. Pap.* **20** (1925) 65.
13. Ginnings, D. C. and Furukawa, G. T. *J. Am. Chem. Soc.* **75** (1953) 522.
14. Furukawa, G. T., Douglas, T. B., McCoskey, R. E. and Ginnings, D. C. *J. Res. Natl. Bur. Std.* **57** (1956) 67.
15. Rossini, F. D., Wagman, D. D., Evans, W. H., Levine, S. and Jaffe, I. *Selected Values of Chemical Thermodynamic Properties, U.S. Natl. Bur. Std. Circular 500,* Washington D.C., 1952.
16. Kelley, K. K. *Contributions to the Data on Theoretical Metallurgy.* XIII. *U.S. Bur. Mines, Bull.* **584**, Washington D.C., 1960.
17. Romanovskii, V. A. and Tarasov, V. V. *Soviet Phys. Solid State* **2** (1960) 1176.
18. Martin, D. L. *Can. J. Phys.* **40** (1962) 1166.
19. Edwards, J. W. and Kington, G. L. *Trans. Faraday Soc.* **58** (1962) 1313.
20. Martin, D. L. and Snowdon, R. L. *Can. J. Phys.* **44** (1966) 1449.
21. Ginnings, D. C. *J. Phys. Chem.* **67** (1963) 1917.

Received November 26, 1966.